Advanced Composite Materials
Publication details, including instructions for authors and subscription information:
http://www.tandfonline.com/loi/tacm20

Influence of fiber volume fraction on dynamic damage in woven glass fabric composites: An experimental study

S. Ravi , N. G. R. Iyengar , N. N. Kishore & A. Shukla

Version of record first published: 02 Apr 2012.

To cite this article: S. Ravi , N. G. R. Iyengar , N. N. Kishore & A. Shukla (2000): Influence of fiber volume fraction on dynamic damage in woven glass fabric composites: An experimental study, Advanced Composite Materials, 9:4, 319-334

To link to this article: http://dx.doi.org/10.1163/15685510052000138

Adv. Composite Mater., Vol. 9, No. 4, pp. 319–334 (2000)

Influence of fiber volume fraction on dynamic damage in woven glass fabric composites: An experimental study

S. RAVI [1,*], N. G. R. IYENGAR [1], N. N. KISHORE [1] and A. SHUKLA [2]

[1] *Indian Institute of Technology, Kanpur-208016, India*
[2] *University of Rhode Island, Kingston, RI 02881, USA*

Received 17 February 2000; accepted 30 July 2000

Abstract—Experiments have been carried out to study the damage fracture growth and the associated damage mechanisms in woven glass fiber reinforced polyester composites. The initiation and propagation history of the damage has been recorded at few microsecond intervals using a high speed Cranz–Schardin camera. The images obtained are analyzed using IDRISI, an image processing tool. Three different fiber volume fractions, 2.4, 5.3 and 33.0 percent are considered. The influence of notch orientation are studied by varying the initial notch orientation between 0° and 45°. On the basis of the studies, it is observed that irrespective of initial notch orientation, the damage propagates in a direction perpendicular to the loading direction. For low fiber volume fractions, the damage is in the form of matrix cracking and interface debonding while delamination dominates for specimens with high fiber volume fractions. The damage velocity in low fiber volume fraction specimens are found to be higher than the terminal velocity of the crack in unreinforced polyester resin. Fractographic studies are also carried out and the results are presented.

1. INTRODUCTION

Fiber reinforced polymeric composite laminates have been used extensively in aircraft, automobile industries and in civil engineering structures. These structures may be subjected to different type of loads which are either static or dynamic in nature. Of primary importance, as regard to the integrity and safety of composite structures, is the complete understanding of the damage and failure processes that occur in these materials. Static fracture of composite materials has been extensively studied and reported in the literature [1]. Dynamic impact behaviour has also been

[*]To whom correspondence should be addressed at Room No. 513, Research Institute for Applied Mechanics, Kyushu University, 6-1 Kasuga-koen, Kasuga, Fukuoka 816-8580. E-mail: ravi@riam.kyushu-u.ac.jp

well investigated and reported [2]. However, very little work has been reported on the dynamic fracture of composite materials. Shukla and Khanna [3] have studied the effect of introducing the fibers on dynamic crack growth in brittle matrix and the damage growth behaviour when a fast moving crack interferes with strong fibers. They also studied the effect of fiber orientation and the interfacial bond strength between fiber and matrix [4]. It was shown that the presence of fiber with weak bonding reduces the fracture energy available at the crack tip which results in a smaller crack jump distance. Agarwal *et al.* [5] used commercially available fiber reinforcements as opposed to the discrete fibers used in Ref. [3], to study the dynamic damage growth in glass/polyester composites. They observed that, similar to static growth, the damage zone generally propagates perpendicular to loading direction. Their results show that the velocity of damage propagation is slightly lower than the crack propagation velocity in unreinforced polyester resin. The aim of the work reported in this paper is to study the dynamic damage growth in glass–polyester composites. Damage growth patterns have been obtained at few microsecond intervals for the different composites studied. The image obtained are analyzed to get a good understanding of various phenomena.

Most of the work found in the literature is on unidirectionally reinforced composites. Recently woven fabrics are finding wider application because of (i) ease of handling, which lends itself to automation and consequent reduction in labour, (ii) the ability of fabric to conform to complex shapes and the fact that the in-plane properties of fabric are closer to isotropic than those of unidirectional fibers. Further, Curtis and Bishop [6] have shown that delamination and certain forms of matrix cracking can enhance the residual tensile properties of a notched woven carbon fiber composites under static loading. Therefore, it will be of interest to study the composites reinforced with woven glass cloth fabric under dynamic loads. In our earlier study on dynamic damage growth in glass cloth/polyester composites [7], it has been observed that the damage zone consisting mainly of debonding and matrix cracking, propagates perpendicular to the loading direction. In the present study, a similar composite system has been used to investigate the effect of (i) fiber volume fraction and (ii) initial notch orientation under dynamic loads.

2. MATERIAL AND SPECIMEN PREPARATION

2.1. Material

Transparent glass/polyester composite plates have been fabricated in the laboratory to study the damage growth behavior under dynamic loads. The reinforcement in the form of woven glass cloth with a balanced weave (Harsh-Deep Industries, Ahmedabad 380023, India), and clear sheet grade polyester resin (Parikh Chemicals, Kanpur 208016, India) as matrix have been used. The polyester resin is added with Divinyl benzene (2 wt%) and dibutyl phthalate (5 wt%) to match its refractive index with that of the glass fiber and then cured with 1 wt% methyl ethyl ketone

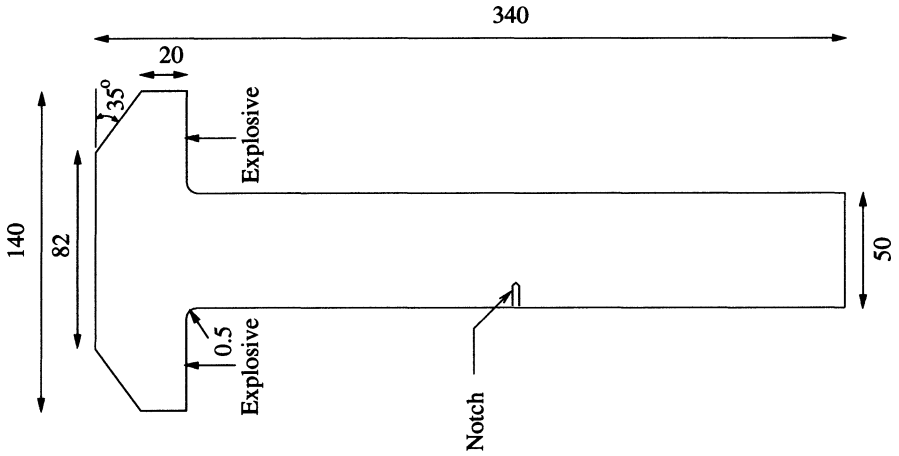

Figure 1. Overall specimen geometry with dimensions (all dimensions are in mm).

peroxide and 0.3 wt% cobalt octate. The composite plates are cast in between two mylar lined plexi-glass sheet mould. The composite plates are cured at room temperature for 24 h followed by a post-curing at 80°C for 8 h. Composite plates fabricated thus with 33% fiber volume fraction (V_f) show a maximum transmission ratio of 69.5% at 589 nm.

2.2. Specimen

The modified single edge notched (MSEN) specimen used for the present study is shown in Fig. 1. The specimen configuration and dimensions are selected such as to achieve plane loading stress waves in the notch plane. To ensure the plane nature of the loading pulse, FEM simulation has been carried out.

2.2.1. FEM simulation. The hyperbolic equation representing elastic wave propagation in a homogeneous, anisotropic and linear elastic solid, in the absence of body forces, can be written as,

$$C_{ijkl}u_{k,lj} = \rho\ddot{u}_i. \tag{1}$$

The total potential of such a linear elastic body can be expressed, using D'Alembert's principle, as

$$\Pi = \frac{1}{2}\int_V u_{i,j}\sigma_{ij}\,\mathrm{d}V - \int_{S_t} u_i t_i\,\mathrm{d}S + \int_V u_i\rho\ddot{u}_i\,\mathrm{d}V, \tag{2}$$

where the first term corresponds to the strain energy, the second term to the work done by the surface traction t_i and the last term signifies the work done by the inertia forces. V and S_t denote volume and surface of the domain over which the integration is to be carried out. The finite element solution involves discretization of the domain into suitable finite elements connected to each other at the nodes.

Using standard procedure for discretization [8], the above equation can be rewritten in terms of nodal values of elements as:

$$[M]\left\{\frac{\partial^2 u}{\partial t^2}\right\} + [K]\{u\} = \{F\}, \tag{3}$$

where $[M]$, $[K]$ and $\{F\}$ respectively are the global mass matrix, the global stiffness matrix and the applied load vector. In terms of elemental matrices, they can be expressed as:

$$[M] = \sum_e \int_{V_e} \rho [N]^T [N] \, \mathrm{d}V, \quad [K] = \sum_e \int_{V_e} [B]^T [D][B] \, \mathrm{d}V,$$
$$\{F\} = \sum_e \int_{S_e} [N]\{t\} \, \mathrm{d}S. \tag{4}$$

Both the stiffness and mass matrices are large, sparse, symmetric and positive definite and are effectively stored by the *skyline storage scheme*. Equation (3) is solved by time integration technique and for the present analysis, *Newmark's average acceleration scheme* has been used.

The domain (as shown in Fig. 1) has been discretized uniformly with bilinear quadrilateral isoparametric elements as suggested by Seron *et al*. [9]. The system of linear, second order, ordinary differential equations with constant coefficients are to be integrated in the time interval $(0, T)$ at discrete time steps. Thus the equations

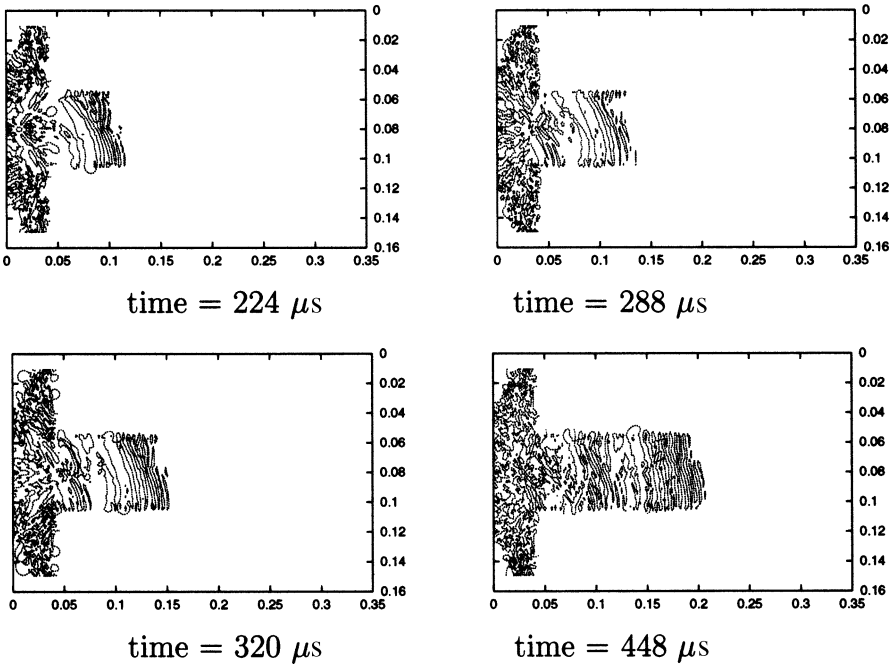

Figure 2. Stress wave propagation in the MSEN specimen (FEM).

are integrated at every t_n where the time variable $t_n = n\Delta t$, $0 \leqslant n \leqslant N$, and $\Delta t = T/N$. The discretization, however, is not arbitrary and has to satisfy certain stability norm as explained in Ref. [8].

The dynamic load is modeled as

$$F = \begin{cases} \left[\frac{P_{\max}}{0.36788}\right]\left[\frac{t}{t_{\max}}\right]\exp\left(\frac{-t}{t_{\max}}\right) & 0 \leqslant t \leqslant T \\ 0 & t > T. \end{cases} \tag{5}$$

The stresses produced due to the dynamic load are plotted as stress contours and this is shown in Fig. 2. It is seen that the stress waves become planar when they reach the notch plane, which is approximately 150 mm from the modified end. It has also been established through experiments that the stress waves travelling in the test area (notch plane) form a plane fronted tensile wave [7].

3. EXPERIMENTAL TECHNIQUE

Dynamic damage growth in fiber composites has been studied using modified single edge notched (MSEN) specimens. The specimen is placed on the optical bench of a Cranz–Schardin type high speed camera as shown schematically in Fig. 3 and subjected to dynamic loading. Dynamic loads are produced by the simultaneous detonation of two explosive charges (50 mg of PETN) on both the side-shoulders of the specimen. Damage in the form of debonding, fiber breakage, matrix cracking, etc. make the transparent composite specimen locally opaque. Hence, the initiation and propagation of damage can be recorded by photographing the specimen sequentially at a predetermined short time intervals (5 μs) using the Cranz–Schardin high speed camera. The light produced in the open-air spark gap is focused onto the specimen using fiber optic cables. The three-dimensional damage processes that take place in the composite specimen are projected onto the 2D image plane using the two field lenses of the optical bench as shown in the Fig. 3. The oscilloscope record of the light intensity sensed by the ultra high speed photodiode provides the actual firing time of the individual frames.

A Cranz–Schardin camera provides a sequence of twenty discrete images in the predetermined intervals of time. These images were digitized and processed to obtain the damage zone size information. An image processing tool, IDRISI has been used to process these images to get the damage zone area and length informations. Stereo Microscope and Scanning Electron Microscope (SEM) have been used to investigate the surface of the damaged specimens.

The composite specimen having the overall dimensions as shown in Fig. 1 was cut using a router guided by a template. Initial notches have been cut using a slitting saw cutter which has V-shaped cutting edge with 60° included angle. For the present study, 0°, 15°, 30° and 45° notch orientations with respect to horizontal are considered. The crack length to specimen width (a/w) ratio of 0.25 has been

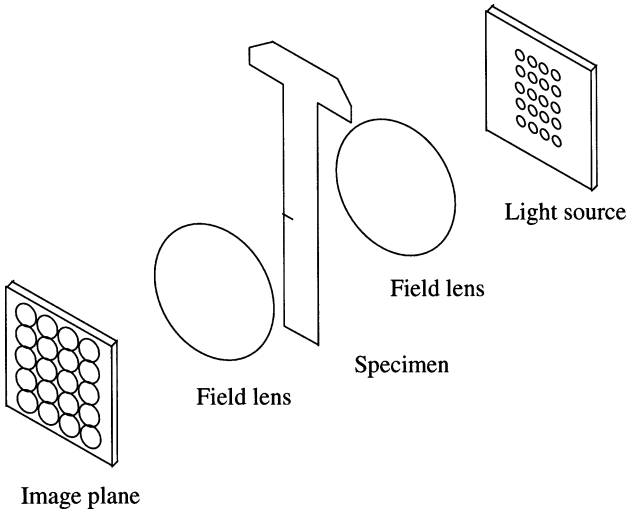

Figure 3. Optical bench arrangement for investigating damage process in composites under explosive generated tensile load.

used for all the specimens. The notch angles other than 0° are cut by keeping the notch tip at the same location.

4. RESULTS AND DISCUSSION

4.1. Effect of fiber volume fraction on damage growth

Typical damage initiation and propagation history observed in single layer (V_f = 2.4%), two layer (V_f = 5.3%) and ten layer (V_f = 33%) composite specimens are shown in Figs 4, 5 and 6 respectively. From these figures, it is observed that the damage growth is perpendicular to the loading direction and parallel to the notch plane, as observed in homogeneous materials. However, in composites, the damage is due to many micromechanisms which include matrix cracks, fiber–matrix interface debonding and delamination. In homogeneous materials, a single crack propagates with possible crack branching under appropriate loading conditions [10–12]. In composites, a damage zone is formed due to multi-directional microcracks in the matrix (Fig. 7) and at the interfaces between fiber and matrix and between layers. The damage initiates at the notch tip and propagates perpendicular to the loading direction. During this propagation, the lateral dimension (width) of the damage adjacent to the notch also increases.

Another feature observed in low fiber volume composite specimens is the *damage zone splitting*, similar to crack branching in unreinforced polymer materials. Microscopic observation reveals crack branching in the matrix region also. Figure 7 delineates the damage zone, consisting of matrix microcracking, crack branching in the matrix zone and also the debonded zone (bright area) in single layer composite.

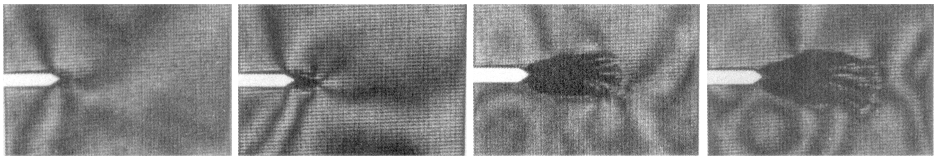

Figure 4. Damage growth pattern in single layer ($V_f = 2.4\%$) composite MSEN with 0° notch (the photographs also show isochromatic fringe patterns).

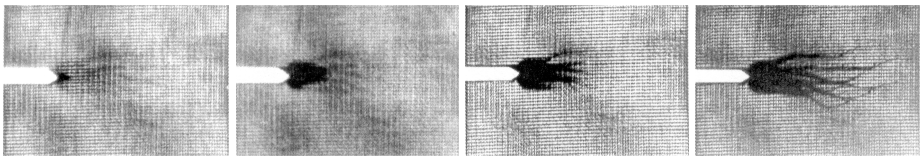

Figure 5. Damage growth in two layer ($V_f = 5.3\%$) composite MSEN specimen with 0° notch.

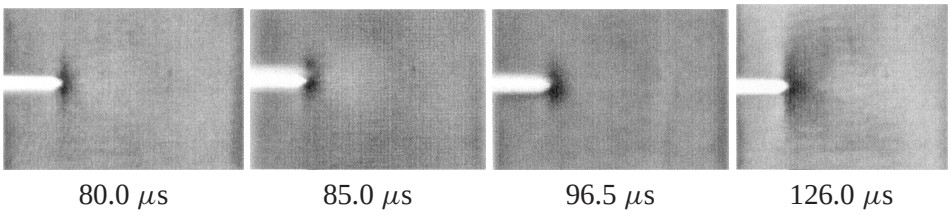

Figure 6. Damage growth pattern in 10 layer ($V_f = 33.0\%$) composite MSEN with 0° notch.

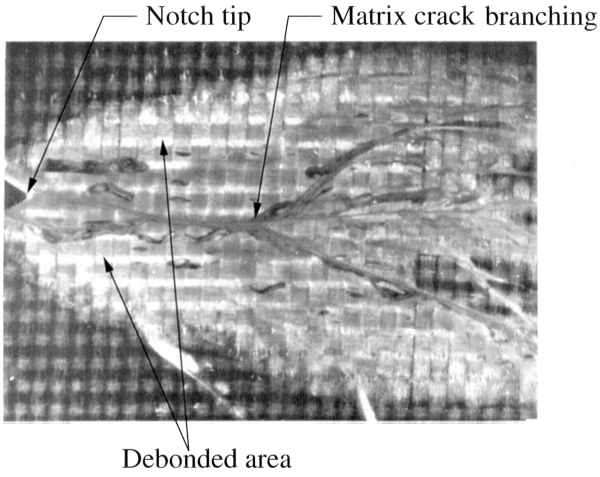

Figure 7. Microscopic picture showing the debonded area and matrix crack with branching in single layer ($V_f = 2.4\%$) composite specimen with 0° notch.

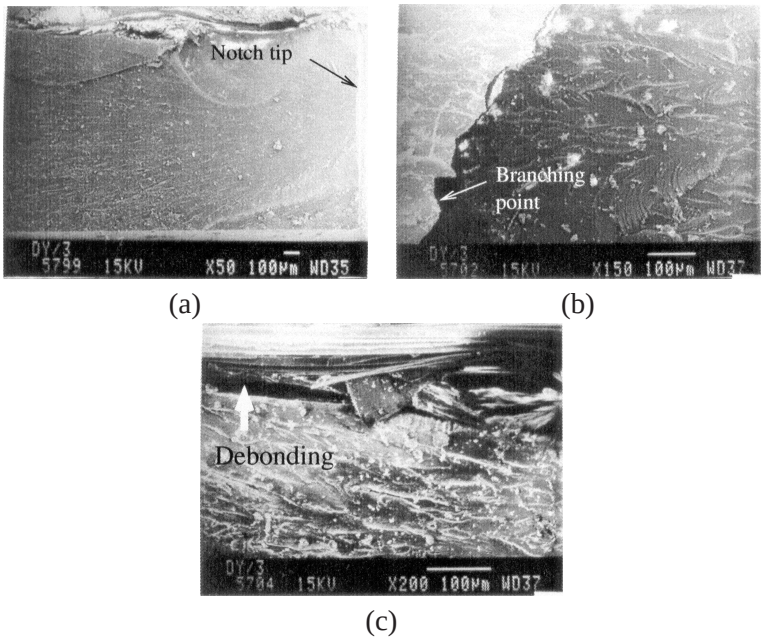

Figure 8. SEM photographs showing the fracture surface (a) at the notch tip (b) just before branching (c) fiber–matrix interface debonding in single layer composites ($V_f = 2.4\%$).

Further, for low V_f, a single matrix crack is initiated from the tip of the notch which is then branched out. Many matrix cracks, neither connected to the initial notch nor the main crack, are also seen near the notch.

The crack surface morphology for various fractured specimens are shown in Figs 8, 9, 10 and 11. In single layer composite specimens, the fracture surface on the matrix region just after initiation is smooth but becomes rough afterwards (Fig. 8a). Finger like striation fanning out can be seen in this rough region. The surface is extremely rough at the site of matrix crack branching (Fig. 8b) which indicates the energy available for the propagation is in excess than required for the propagation. This excess energy is expended in splitting up the matrix crack and also the damage zone. Figure 8c shows the fiber–matrix interface failure observed in single layer composite specimens.

The microscopic pictures of the fractured surface of two layer composite show some interesting features. Figure 9 shows the fracture surface during damage initiation in a two layer composite specimen. It can be seen that the fracture is matrix dominated, as observed in single layer composites. The initiation seems to be independent in the three regions of matrix separated by the two layers of reinforcement. In the matrix region on either side, groups of striation fanning out could be seen. This feature has been observed in single layer composites also (cf. Fig. 8). It is observed that these striation markings are less dense in the middle matrix region. But, as the damage propagates, the fractured surface becomes featureless on the top and bottom surface matrix regions and dense striation could

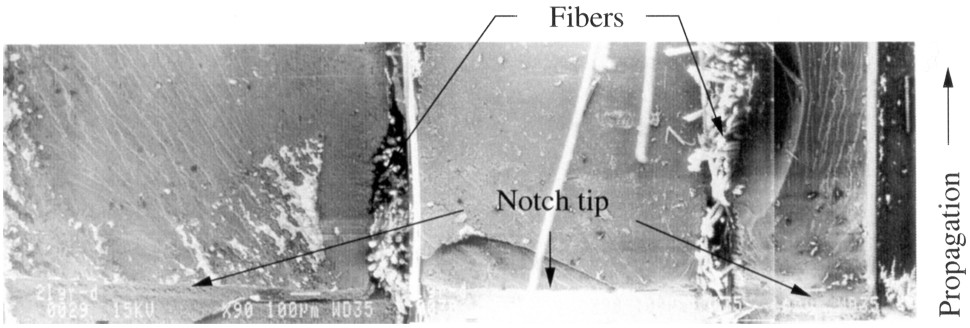

Figure 9. Microphotograph showing the fractured surface at the initiation site in two layer (V_f = 5.3%) composites.

be seen in the central region which is constrained by the fibers on either side. These striations are seen all along the propagation up to the arrest. Another feature observed is the matrix cracking in the thickness direction (cf. Fig. 10). A similar crack (i.e. across the width of the specimen) has been observed in single layer composite (cf. Fig. 8b). In the case of a two layer composite specimen, because of the presence of the reinforcement on either side, the crack developed in the middle matrix zone could not travel to the entire width of the specimen for a successful matrix branching. Therefore, this region may be the source of branching. The optical microphotograph shown in Fig. 10 delineates the matrix crack observed in the middle matrix region. The fast moving matrix crack may be trying to extend to the entire width, but the presence of fibers causes the crack to propagate in the interface leading to interface failure.

The initial damage velocity in single and two layer composites are found to be 460 and 490 m/s respectively. These values are higher than the terminal velocity, 432 m/s of polyester resin [11]. This could be due to the higher stress wave velocities in glass fibers as compared to the resin. Due to these higher stress wave velocities, the energy gets transferred to the damage initiation sites faster than in pure resins. Further, under such high velocity, one can expect the damage zone split to occur forming a rough fracture surface.

As the fiber volume fraction increases, it is found that specimens even with 70% transmission ratio are not good enough for damage propagation studies, as all the details are not clearly seen. Figures 6 and 17 show the photographs of the damage history in specimens having $V_f = 33\%$ with a 0° and 15° notch, respectively. The damage mechanism changes as the fiber volume fraction increases. While a single matrix crack initiated in specimens with low fiber volume fraction, multiple matrix cracks all around the notch, with the main crack originating form the notch tip can be seen in specimen with $V_f = 33\%$. The optical microphotograph, Fig. 11a, show the multiple cracks in a ten layer composite specimen. Further, the SEM photograph of the fractured surface of the ten layer composite specimen shows a large delamination zone indicating that, for higher V_f, the fracture is no longer a matrix dominated one. The energy absorbing mechanism appears to be the damage

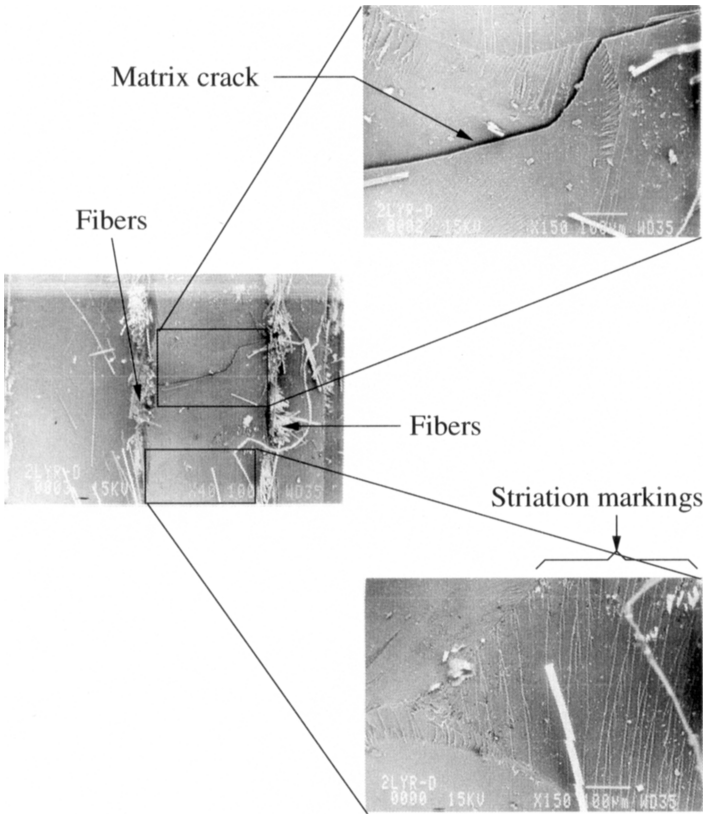

Figure 10. SEM photograph showing the crack in the middle matrix zone of two layer ($V_f = 5.3\%$) composites.

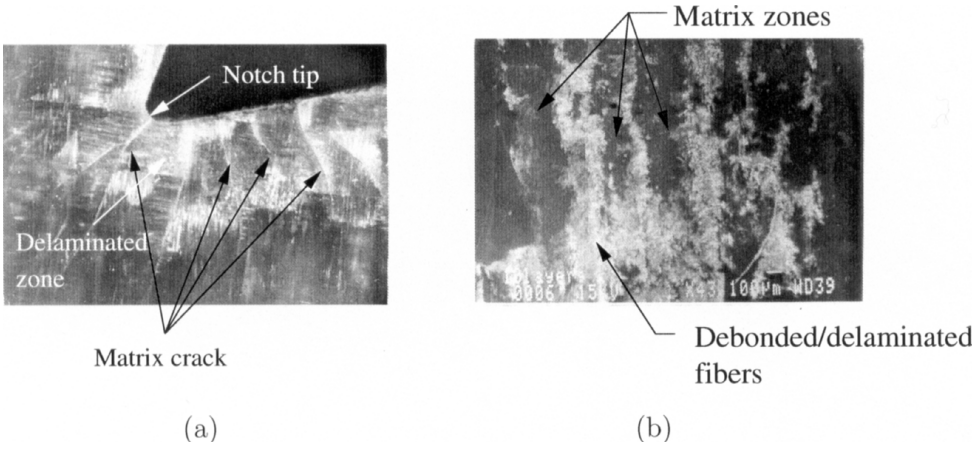

Figure 11. Damage zone in ten layer ($V_f = 33.0\%$) composite specimen. (a) Multiple matrix cracks at the notch tip and (b) SEM photograph showing the delaminated and debonded fibers as bright spots.

in the form of delamination and debonding of the fiber–matrix interface. The delaminated or debonded fibers are shown as bright spots in Fig. 11b. The matrix region is relatively featureless and smooth.

For low V_f, the damage initiated with matrix cracking followed by fiber–matrix debonding, matrix crack branching and damage zone splitting. On the other hand, for higher V_f, matrix cracking is followed by fiber–matrix debonding and delamination. In all the cases studied, no fiber breaks have been observed. For a given energy, it is observed that damage size reduces as the V_f increases. Also, for low V_f, a single matrix crack initiated which is then branched out, while at high V_f, multiple cracks are initiated around the notch tip with a main crack originating from the tip.

4.2. Effect of notch orientation

The damage velocity and size are influenced by the initial notch orientation. Figures 12 to 16 show the damage growth in single and two layer composites with 15°, 30° and 45° notch orientations. Figure 17 shows the damage growth in a ten layer composite with 30° notch orientation. It is seen from these figures that, irrespective of notch orientation, the damage zone size reduces as the fiber volume fraction increases. Damage zone splitting can be observed in almost all cases except

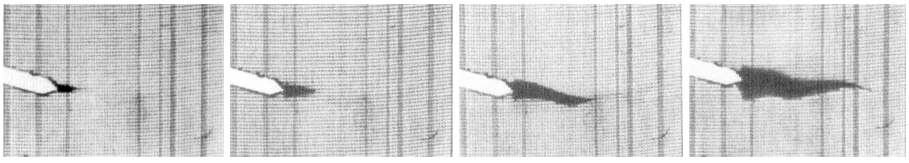

Figure 12. Damage growth pattern in single layer ($V_f = 2.4\%$) composite MSEN with 15° notch.

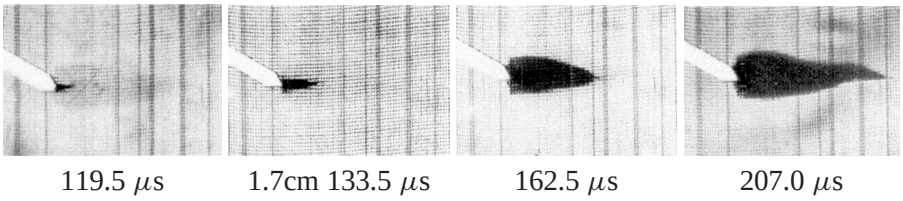

Figure 13. Damage growth pattern in single layer ($V_f = 2.4\%$) composite MSEN with 30° notch.

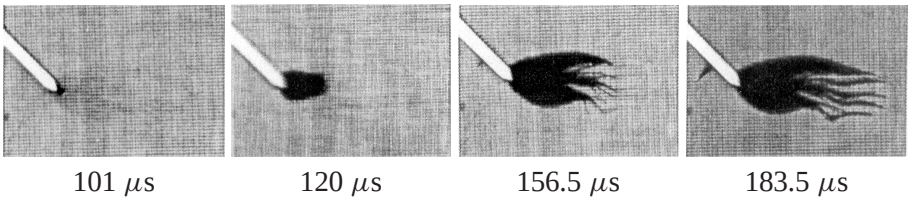

Figure 14. Damage growth pattern in single layer ($V_f = 2.4\%$) composite MSEN with 45° notch.

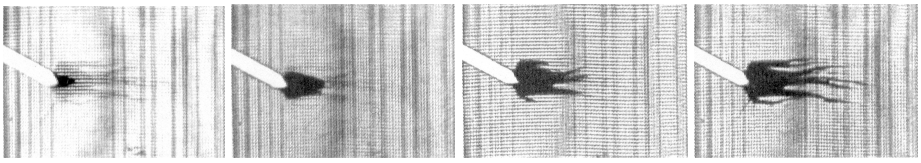

Figure 15. Damage growth pattern in 2 layer ($V_f = 5.3\%$) composite MSEN with 30° notch.

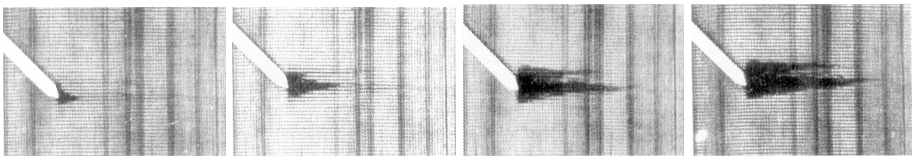

Figure 16. Damage growth pattern in 2 layer ($V_f = 5.3\%$) composite MSEN with 45° notch.

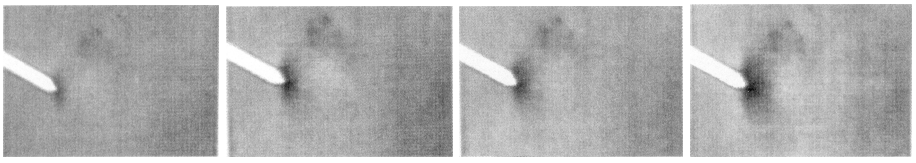

Figure 17. Damage growth pattern in 10 layer ($V_f = 33.0\%$) composite MSEN with 30° notch.

in Figs 12 and 13. In all cases studied, the damage initiated with matrix cracking followed by fiber–matrix debonding, as observed in 0° notched specimens. No fiber breaks could be observed.

The velocity of the damage propagation has been computed by plotting the relative position of the transverse damage size (maximum dimension) with respect to time. Figure 18 shows the relative position of the damage tip with respect to time for all the specimens considered. A quadratic curve seems to fit the data. The slope of this plot gives the speed at which the damage propagates. From Fig. 18a and b, it is observed that in single layer composites, the damage initiation time increases with notch orientation up to 30°. However, for the 45° notch, the damage initiated much earlier. On the other hand, the damage initiation time is almost the same for all notch orientations considered in the case of two layer composites. Table 1 gives the propagation velocity of the damage for different specimens. It is observed that the initial velocity is approximately same for both $V_f = 2.4$ and 5.3 percent. The difference is in the final velocity. While the damage slows down to a lower value in single layer composites, the damage in two layer composites gets arrested eventually. Further, the post-mortem investigations on the specimens revealed that the damage traveled to the entire width of the specimen in single layer composite, which is not seen in other composite specimens. Microscopic pictures show that during these periods, only matrix cracks without fiber/matrix debonding and also

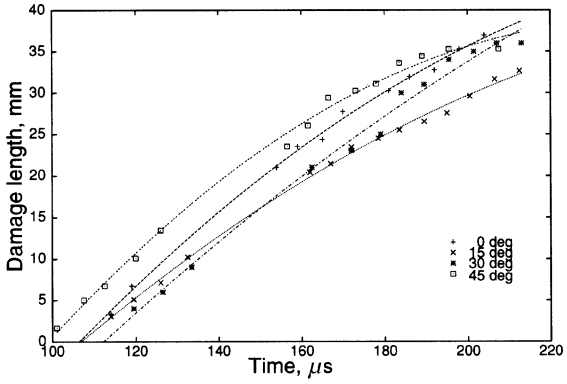

(a)

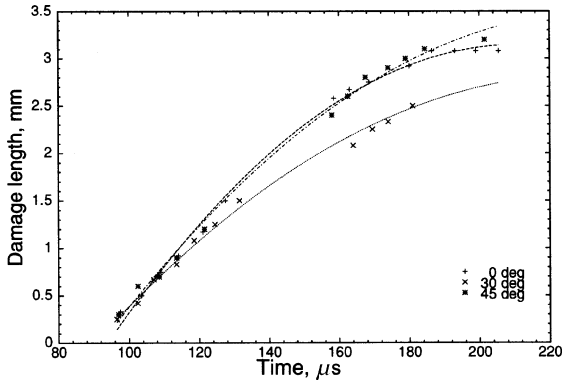

(b)

Figure 18. Relative position of damage tip during observation period (a) single layer ($V_f = 2.4\%$) and (b) two layer ($V_f = 5.3\%$) composites.

Table 1.
Damage propagation velocity and rate of growth of damage in glass/polyester composites

Volume fraction	Notch orientation	Velocity (m/s)		Rate of growth (m^2/s)	
(%)	(deg)	Initial	Final	Initial	Final
2.4	0	460	260	3.49	—
	15	400	210	3.35	—
	30	420	320	3.21	—
	45	470	150	3.42	—
5.3	0	490	0	2.50	0.45
	30	380	0	2.22	0.13
	45	450	0	2.92	0.98

some of the branched cracks gets arrested, as can be seen in Fig. 19. This lowering of velocity and arrest is due to the unloading of the damage zone as the trailing part of the stress wave passes over.

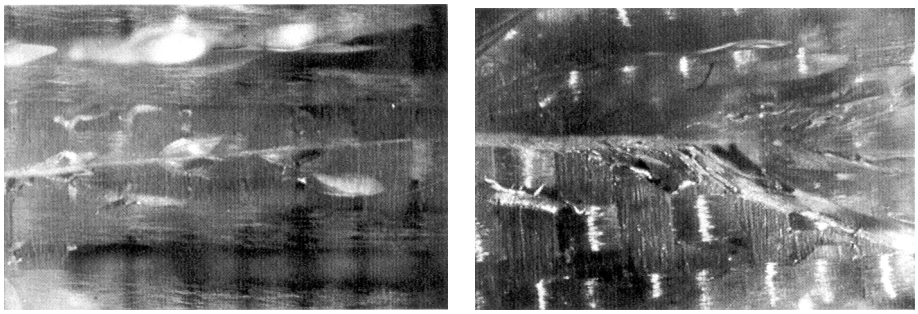

Figure 19. Attempted branching and the successful branching observed in two layers ($V_f = 5.3\%$) composites.

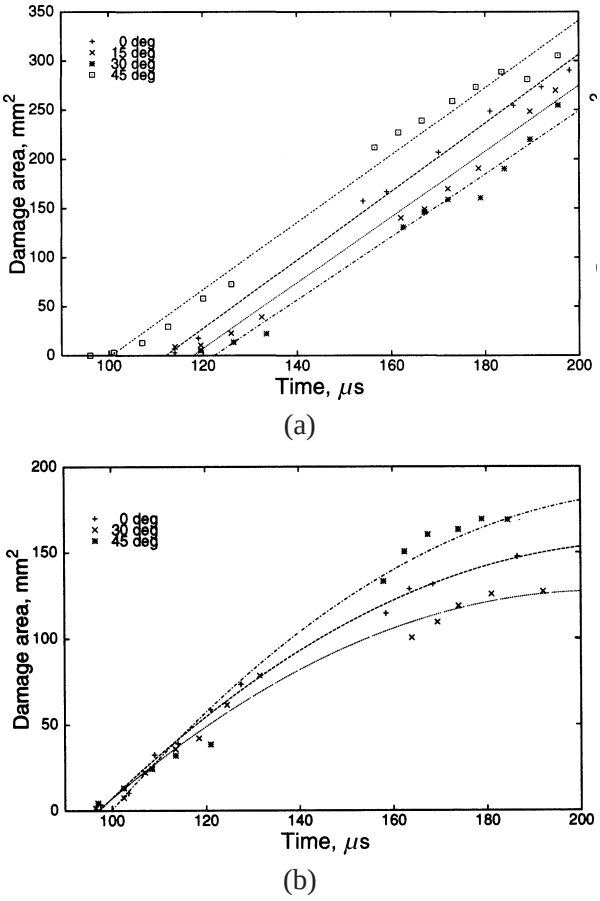

Figure 20. Propagation of damage zone during the observation period (a) single layer ($V_f = 2.4\%$) and (b) two layer ($V_f = 5.3\%$) composites.

Figure 20a and b show the damage size with respect to time respectively for single and two layer composites. Table 1 also gives the damage growth rate on these

composites. From these figures and the Table, it is observed that the damage grows at a faster rate in single layer composites compared to that of two layer composite specimens. It can be seen from Fig. 20a that the damage grows almost at a constant rate during the observation period while in two layer composites, the damage slows down at the end of the observation period and eventually gets arrested. Lower fiber volume fraction implies lower resistance and therefore the higher damage velocity in single layer composites. As the fiber volume fraction increases, the resistance also increases. Because of this higher resistance, even though the initial damage speed in two layer composites is of the same order of magnitude as observed in the single layer composites, the damage does not propagate at constant velocity. Its slows down in the later part of the observation period. When viewed under the stereo microscope, the attempted branching in matrix crack could be seen with the final successful branching (Fig. 19). This type of behaviour is not observed in the single layer composites specimen.

5. CONCLUSIONS

The damage growth in glass fiber reinforced polyester matrix has been investigated. Three different fiber volume fractions, 2.4, 5.3 and 33.0 percent, are considered. The influence of notch orientation on damage has been studied. On the basis of the studies carried out, the following conclusions can be drawn:

1. The finite element simulation studies carried out show that the waves loading the notch is planar.
2. The damage propagates in a direction perpendicular to the loading direction irrespective of notch and fiber orientations.
3. The damage initiates with the matrix crack followed by debonding and delamination.
4. No fiber breaks could be observed.
5. The damage velocity in composites is higher than the terminal velocity of polyester matrix for similar geometries. Under such high velocities, the damage zone splits, like the crack branching in polymer materials.
6. For a given energy, the damage area reduces as the fiber volume fraction increases.
7. Notch orientation affects the damage area and velocity: they reduce with increasing notch orientation up to 30°. However, for a 45° notch, these are the highest.

Acknowledgements

The partial support from the National Science Foundation under grant number INT-971494 to Indian Institute of Technology, Kanpur, India and INT-9700670 to the

University of Rhode Island, USA, and the financial support to one of the authors (Ravi) from Aeronautics Research and Development Board (Structures panel), Government of India to carry out this work are gratefully acknowledged.

REFERENCES

1. B. D. Agarwal and L. J. Broutman, *Analysis and Performance of fiber composites*. John Wiley, New York (1990).
2. S. Abrate, *Impact on composite structures*. Cambridge University Press, Cambridge, U.K. (1998).
3. A. Shukla and S. K. Khanna, Effect of fiber reinforcement on dynamic crack growth in brittle matrix composites, *Trans. ASME J. Engng Mater. Technol.* **115**, 140–145 (1993).
4. S. K. Khanna and A. Shukla, Influence of fiber inclination and interfacial conditions on fracture in composite materials, *Exper. Mech.* **34**, 171–180 (1994).
5. B. D. Agarwal, R. Sharma and K. K. Bajpai, Experimental study of crack induced dynamic damage growth in fiber composites, *Mech. Compos. Mater. Struct.* **2**, 295–308 (1995).
6. P. T. Curtis and S. M. Bishop, Fractography of unfilled and particulate-filled epoxy resins, *Composites* **15**, 259–265 (1984).
7. S. Ravi, N. G. R. Iyengar, N. N. Kishore and A. Shukla, Experimental studies on damage growth in composites under dynamic loads, *Appl. Compos. Mater.* (accepted for publication).
8. K. J. Bathe and E. L. Wison, *Finite Element Procedures*. Prentice-Hall, Englewood Cliff, N.J. (1996).
9. F. J. Seron, F. J. Sanz and J. I. Badal, Finite element method for elastic wave propagation, *Comm. Appl. Neumer. Meth.* **6**, 359–368 (1990).
10. K. Ravi-Chandar and W. G. Knauss, An experimental investigation into dynamic fracture: III On steady-state crack propagation and crack branching, *Intern. J. Fract.* **26**, 141–154 (1984).
11. J. W. Dally, Dynamic photoelastic studies of fracture, *Exper. Mech.* **19**, 349–361 (1979).
12. A. Shukla, H. Nigam and H. Zervas, Effect of stress field parameters on dynamic crack branching, *Engng Fract. Mech.* **36**, 429–438 (1990).